Stochastic modelling of turbulent flows for numerical simulations

Carlo Cintolesi, Etienne Mémin

Theoretical and Computational Fluid Dynamics manuscript No.
(will be inserted by the editor)

Stochastic modelling of turbulent flows for numerical simulations

Carlo Cintolesi · Etienne Mémin

Received: date / Accepted: date

Abstract The stochastic model proposed by Mémin [24] for turbulent flow simulations is analysed, both theoretically and numerically. It is shown to be a generalisation of the classical large-eddy simulation approach, and to describe a richer physics. The model does not lead to the eddy-viscosity assumption and can be reduced to Smagorisky model under restrictive hypotheses; hence, it can be considered as a generalisation of classical models. Simulations of a turbulent channel flow at $Re_\tau = 590$ shows the presence of physical phenomena usually not reproduced; namely a weak turbophoresis and of a turbulent compressibility linked to streaks structures. The turbulent kinetic energy budget suggests that the model is more effective in dissipating energy near the wall. For the sake of completeness, alternative and detailed derivation of the stochastic model is reported in detail in the appendix.

Keywords Stochastic models · Turbulence modelling · Numerical simulations · OpenFOAM.

1 Introduction

The reliable numerical simulation of turbulent flows is still nowadays a challenging issue, both in terms of mathematical modelling and of computational cost required. In the last decades, different techniques were developed to tackle this problem, the most fruitful for practical applications being the Reynolds-averaged simulation and the Large-Eddy Simulation (LES) methodologies. Despite the continuous improvements with increasingF accuracy of the models,

C. Cintolesi
INRIA Rennes, Fluminance group, Campus de Beaulieu, F-35042 Rennes (France)
E-mail: carlo.cintolesi@gmail.com

E. Mémin
INRIA Rennes, Fluminance group, Campus de Beaulieu, F-35042 Rennes (France)
E-mail: etienne.memin@inria.fr

such methodologies are developed within a deterministic framework. Hence, they cannot completely represent the random nature exhibited by turbulent flows, that eventually requires the use of stochastic calculus. In the field of geophysical flows, probabilistic models are used to correct the effects of the coarse spatial discretisation. Similarly, the stochastic variables can be employed to account for the unresolved processes in the numerical reproduction of engineering and environmental flows.

The literature proposes different approaches on this topic. The stochastic Langevin equation is derived assuming that a fluid-particle velocity is perturbed by a Brownian motion, which is found to well described the dynamics of turbulent flows; see Pope [35]. This equation was used in the framework of Probability Density Function (POF) methods to reproduce homogeneous isotropic turbulence, but also inhomogeneous and anisotropic turbulence by Pope [36] and by Durbin & Speziale [8], respectively. Orszag [33] and Leslie [22] introduced the Eddy-Damped Quasi-Normal Markovian (EDQNM) models; see the overview by Lesieur [21]. The large-scale equations were closed in spectral space through a Gaussian closure. They were particularly suitable to study strong non-linearity in the small-scale turbulence. In the same framework, Chasnov [5] develops a forced-dissipative model, where the large-eddy Navier-Stokes equations were corrected by a stochastic force terms. This was a Gaussian forcing uncorrelated in time, homogeneous and isotropic in space. Kraichnan [16] exploits a different approach: the momentum equations are replaced by a set of equations with same mathematical properties, which are closed using a Gaussian stochastic model. This theory leads to valuable results in terms of mathematical properties (existence, singularities) and physical effects (turbulent diffusion, backscatter) analyses. Frederiksen [11] shows that the same strategy can be used for a stochastic modelling of barotropic flows or in quasi-geostrophic approximation, that includes the interaction between topography and small-scale eddies. The randomness effects can be also explicitly introduced by means of *ad hoc* stochastic terms. Investigating the plane shear mixing layer, Leith [20] improves the accuracy of LES with Smagorinsky model by introducing an explicit stochastic terms. On the theoretical side, Flandoli [9] studied fluid dynamic systems corrected with a random white noise force to reproduce the complex phenomena related to turbulence.

These attempts have some limitations: the POF and EDQNM models required to work in the spectral space instead of the physical one; there is a certain degree of arbitrariness when explicit random terms are introduced (e.g. the random forcing should be multiplicative or additive); and overall the models can be hardly generalised for practical applications.

The methodology here presented aims to overcome these shortcomings. It develops from a different starting point: the fluid-particle trajectory in the Lagrangian framework is assumed to be a random process. It is expressed by a semimartingale, where the finite-variation part represents the smooth macroscopic velocity, while the martingale models the perturbations due to the turbulent motion. Consistently, an expression of the velocity is found and stochastic calculus is used to derived the stochastic equations of motions. In

such a procedure, the use of the Itō-Wentzell formula is crucial to compute the time derivative, see Kunita [18]. A first work in this direction was that one of Brzeźniak [2], subsequently extended by Mikulevicius and Rozovskii [27] and Flandoli [10]. Globally, these works focused on the mathematical properties of the stochastic equations. The work of Mémin [24] follows a similar approach and developed the so called model under Location Uncertainty (LU), which is oriented to practical application in computational fluid dynamics. Recently, Holm [13] derived a similar set of equations using Lagrangian mechanics, which leads to additional terms, while Neves *et al.* [29] studied theoretically a similar system of equations. The LU model was applied to different applications: Resseguier *et al.* [37,38,39] used it for geophysical flows simulations, where it exhibits a high accuracy in reproducing extreme events and provided new analysis tools. Chapron *et al.* [4] investigated the Lorentz-63 case and found that LU is able to explore the region of the deterministic attractor faster than the classical models. Resseguier *et al.* [40] employed it in conjunction with the proper orthogonal decomposition technique for the numerical simulation of a flow past a circular cylinder at $Re = 3900$.

Although this is a promising methodology, the inherent mathematical complexity of stochastic partial differential equations poses some difficulties: the resolution of stochastic partial equations is not straightforward and can considerably increase the simulation time. For these reasons, Mémin [24] also introduces a simplified model, where the resolution of stochastic equations is avoided by modelling the effects of the random velocity term by physical assumption. This give rise to the so called *pseudo-stochastic simulation* (PSS) methodology: the flow dynamics is described by classical partial differential equations, which includes additional terms provided by the stochastic modeling. The PSS was adopted by Harouna and Mémin [12] to investigate the Green-Taylor vortex flow applying several models for the stochastic contribution. Chandramouli *et al.* [3] employed it to simulate the transitional wake flow with coarse mesh resolution, proving that it generates a more accurate outcomes with respect to classical LES.

Notwithstanding the above mentioned studies, a pointwise analysis of the pseudo-stochastic model is lacking. The aims of the present work is to study in details the characteristics of the LU and the PSS model, both theoretically and numerically, establishing a parallelism with the classical LES methodology. First, a theoretical analysis of the PSS equations is reported; second, a simplified closure model is adopted to perform numerical simulations on the plane channel flow at $Re_\tau = 590$. The simulation outcomes are discussed in light of the previous theoretical analysis and the peculiarity of the PSS are highlighted. The main novelty of this work is to propose a detailed and systematic comparison between PSS and LES approach, pointing out the physical meaning of the extra term arising from the stochastic derivations (supported by simulations). Moreover, after few years from its first formulation, an alternative mathematically derivation of the LU and PSS model is proposed in the appendix. Efforts have been made to simplify and give a linear structure to the procedure, highlighting the key hypotheses.

The paper is organized as follows: section 2 presents the pseudo-stochastic model and the relative turbulent kinetic budget; section 3 reports a physical interpretation of the model and make a comparison with the LES methodology; section 4 describe the closure model for PSS; section 5 discusses the numerical simulation results; section 6 gives some final remarks. In appendix A an alternative and detailed derivation of the stochastic model for turbulent flows is presented.

2 Pseudo-Stochastic Model

In this section, the stochastic formalism and the pseudo-stochastic equations are reported.

2.1 Stochastic formalism

The particle trajectory in a turbulent regime is not completely known because it is subject to some random (turbulent) effects. Consequently, the fluid-particle displacement is described by the stochastic differential equations of the type:

$$dX_t^i(x_0) = w_i(X_t, t)dt + d\eta_t^i(X_t), \tag{1}$$

where the index $i = 1, 2, 3$ indicates respectively the x,y,z-component in space (they are placed at top or bottom indifferently); $X_t^i(x_0)$ is the trajectory followed by a fluid-particle initially located in x_0; w_i is a differentiable function of bounded variation (i.e. equivalent to a deterministic function) that corresponds to the resolved flow velocity; $\eta_t^i = \int_0^t d\eta_t^i$ is a martingale that accounts for the stochastic contributions to the motion. The Einstein summation convention over repeated indexes is adopted. The stochastic contribution is constructed as a combination of a cylindrical Wiener processes $B_t^k(x)$ not differentiable in time, and a differentiable *diffusion tensor* σ_{ik} which acts as an integral kernel:

$$d\eta_t^i(x) = \int_\Omega \sigma_{ik}(x, y, t)dB_t^k(y)\, dy. \tag{2}$$

Notice that the stochastic processes η_t^i are uncorrelated in time and correlated in space by means of the diffusion tensor.

The expression of the velocity field U_i in Eulerian coordinate x is derived from equation (1); it reads:

$$U_i(x, t) = w_i(x, t) + \dot{\eta}_t^i(x), \tag{3}$$

where the second term on the right-hand side expresses the stochastic velocity defined by formula (22). From a physical point of view, w_i is the velocity expected value and $\dot{\eta}_t^i(x)$ represents a noise: a generalised stochastic process that has to be defined in the space of temperate distribution, see Øksendal [31].

The quadratic variation of the diffusion tensor is a quantity of particular interest; it represents the time-variation of the spatial variance of the stochastic increments along time. It is named *variance tensor* and is defined as:

$$a_{ij}(x,t) = \int_{\Omega} \sigma_{ik}(x,y,t)\sigma_{jk}(x,y,t)\, dy. \tag{4}$$

As a function, it is assumed to have all the regularity (differentiable and integrable in time and space) required by computation; as a tensor, it is a pointwise symmetric and semi-positive definite matrix.

2.2 Pseudo-stochastic equations of motion

The stochastic fluid dynamics equations for a Newtonian incompressible fluid are derived in appendix A. The final system (63) is composed by one set of stochastic equations and one of pure deterministic ones. The former allows to find an expression for the variance tensor a_{ij}, which is required for the resolution of the latter. Together, they provide a close system of equations that composes the LU model. Let us not that full stochastic model can be obtained by relaxing the assumption of bounded variation for the resolved velocity (see [37]).

In order to simplify the model by avoiding the resolution of stochastic partial differential equations, the variance tensor a_{ij} is not computed but modelled through physical assumptions. This choice gives rise to a hybrid model where the stochastic contribution on the governing equations is modelled by a deterministic function, and, overall, no stochastic equations have to be resolved. Such model leads to pseudo-stochastic simulation approach. The PSS momentum and continuity equations for incompressible flows reads, respectively:

$$\begin{cases} \dfrac{\partial w_i}{\partial t} + w_j^* \dfrac{\partial w_i}{\partial x_j} = -\dfrac{\partial p}{\partial x_i} + \nu \dfrac{\partial^2 w_i}{\partial x_j \partial x_j} + \dfrac{1}{2}\dfrac{\partial}{\partial x_j}\left(a_{jk}\dfrac{\partial w_i}{\partial x_k}\right) \\ \dfrac{\partial w_i^*}{\partial x_i} = 0. \end{cases} \tag{5}$$

where ν is the molecular viscosity, the modified pressure $p = p_h + \frac{\nu}{3}\frac{\partial w_\ell}{\partial x_\ell}$ is the sum of the hydrostatic pressure and the divergence of the velocity field (which is not solenoidal), and the effective advection velocity w_i^* reads:

$$w_i^* = w_i - \frac{1}{2}\frac{\partial}{\partial x_k} a_{ik}. \tag{6}$$

The terms depending on a_{ij} account for the effects of the Stochastic Unresolved Scales (SUS) of motion, since the variance tensor is a measure of the intensity and the anisotropy of turbulent random velocities.

Notice that system (5) reduces to the classical Navier-Stokes equations when the a_{ij} is the zero matrix, i.e. when the stochastic contributions disappear.

2.3 Resolved kinetic energy budget

The turbulent kinetic energy (TKE) budget of the resolved scales of motion is presented. The resolved velocity is decomposed in a mean and a fluctuating part, respectively:

$$w_i = W_i + w_i', \tag{7}$$

where the capitol letter indicates the averaged field, $W_i = \langle w_i \rangle$. Variance tensor and pressure are decomposed in a similar way: $a_{ij} = A_{ij} + a_{ij}'$ and $p = P + p'$. The (resolved) turbulent kinetic energy $\kappa = w_i' w_i'/2$ budget reads:

$$\begin{aligned}
&\frac{\partial \langle \kappa \rangle}{\partial t} + \underbrace{\left(W_j - \frac{\partial}{\partial x_k}\frac{A_{jk}}{2} \right) \frac{\partial \langle \kappa \rangle}{\partial x_j} + \langle \left(w_j' - \frac{\partial}{\partial x_k}\frac{a_{jk}'}{2} \right) \frac{\partial \kappa}{\partial x_j} \rangle}_{advection} = \\
&= \underbrace{\frac{\partial}{\partial x_j} \left[-\langle p' w_j' \rangle + \left(\nu \delta_{jk} + \frac{A_{jk}}{2} \right) \frac{\partial \langle \kappa \rangle}{\partial x_j} + \langle \frac{a_{jk}'}{2} \frac{\partial \kappa}{\partial x_j} \rangle + \langle \frac{a_{jk}' w_i'}{2} \rangle \frac{\partial W_i}{\partial x_k} \right]}_{transport} \\
&+ \underbrace{\langle \frac{p'}{2} \frac{\partial^2 a_{jk}'}{\partial x_j \partial x_k} \rangle}_{turb.\ compress.} - \underbrace{\left(\nu \delta_{jk} + \frac{A_{jk}}{2} \right) \langle \frac{\partial w_i'}{\partial x_j} \frac{\partial w_i'}{\partial x_k} \rangle - \langle \frac{a_{jk}'}{2} \frac{\partial w_i'}{\partial x_j} \frac{\partial w_i'}{\partial x_k} \rangle}_{dissipation} \\
&- \underbrace{\langle \left(w_j' - \frac{\partial}{\partial x_k}\frac{a_{jk}'}{2} \right) w_i' \rangle \frac{\partial W_i}{\partial x_j}}_{production} - \underbrace{\langle \frac{a_{jk}'}{2} \frac{\partial w_i'}{\partial x_j} \rangle \frac{\partial W_i}{\partial x_k}}_{loss\ to\ SUS}
\end{aligned} \tag{8}$$

The TKE terms are interpreted in light of the classical budget analysis, e.g. see Kundu and Cohen [17]. On the left-hand side, the second and third terms represent the TKE advection by mean and SUS effective advection velocity. On the right-hand side:

- first four terms: transport by pressure, molecular viscosity and turbulent stresses;
- fifth term: turbulent compression/expansion due to SUS;
- sixth and seventh terms: dissipation by molecular viscosity (it can be proven that A_{ij} is positive defined), resolved turbulence and SUS motions;
- eight term: shear production, this term appears in the mean kinetic budget (not shown here) with opposite sign;
- last term: loss due to SUS also present in the mean kinetic energy budget.

The pseudo-stochastic TKE budget reduces to the classical one if the stochastic contribution is negligible $a_{ij} \simeq 0$. It is worth to notice that the production term includes the contribution of the fluctuations of turbulent advection velocity, while the variance tensor plays a role of a turbulent viscosity dissipation tensor.

3 Analysis of pseudo-stochastic model

The expression of fluid-particle displacement (1) states that a particle trajectory is driven by two actors: a differentiable drift velocity and a Brownian process highly fluctuating in time. In the framework of PSS, the drift velocity w_i that can be interpreted as the resolved velocity field, while the random field assembles the residual motion that are fast oscillating stochastic components, possibly anisotropic and non-homogeneous in space.

3.1 Physical interpretation

Recalling the decomposition of the velocity gradient in symmetric and antisymmetric parts, respectively called the strain-rate tensor and the rotation-rate tensor:

$$\frac{\partial w_i}{\partial x_j} = \frac{1}{2}\left(\frac{\partial w_i}{\partial x_j} + \frac{\partial w_j}{\partial x_i}\right) + \frac{1}{2}\left(\frac{\partial w_i}{\partial x_j} - \frac{\partial w_j}{\partial x_i}\right) = S_{ij} + \Omega_{ij}, \tag{9}$$

the pseudo-stochastic Navier-Stokes equation (5) and continuity equation (6) are rearranged as, respectively:

$$\frac{\partial w_i}{\partial t} + \underbrace{\left(w_j - \frac{1}{2}\frac{\partial a_{jk}}{\partial x_k}\right)}_{effective\ advection}\frac{\partial w_i}{\partial x_j} = -\frac{\partial}{\partial x_i}\underbrace{\left(p_h + \frac{\nu}{3}\frac{\partial^2 a_{sk}}{\partial x_k \partial x_s}\right)}_{modified\ pressure} + 2\nu\frac{\partial S_{ij}}{\partial x_j} + \underbrace{\frac{1}{2}\frac{\partial}{\partial x_s}\left(a_{sk}S_{ki}\right) - \frac{1}{2}\frac{\partial}{\partial x_s}\left(a_{sk}\Omega_{ki}\right)}_{diffusion\ due\ to\ SUS}, \tag{10}$$

and

$$\frac{\partial w_i}{\partial x_i} = \underbrace{\frac{1}{2}\frac{\partial^2 a_{jk}}{\partial x_j \partial x_k}}_{turb.\ compr.}. \tag{11}$$

The terms that depend on variance tensor account for the influence of the SUS on the resolved scales. A physical interpretation of such terms is proposed:

Effective advection: the advection velocity is corrected by an inhomogeneous turbulence contribution. It corresponds to a velocity induced by the unresolved turbulent motions, that can be linked to the *turbophoresis* phenomenon detectable in geophysical flows; i.e. the tendency of fluid-particle to migrate in the direction of less energetic turbulence (see also [37]).

Modified pressure: the non-solenoidal velocity field leads to the presence of an isotropic turbulent factor, that has the dimension of a pressure: $p_t = \frac{\nu}{3}\frac{\partial^2 a_{sk}}{\partial x_k \partial x_s}$. This term does not contribute to the flow and it is included in the pressure gradient in the same manner as the isotropic residual stress in the Smagorinsky model, see [35].

Diffusion due to SUS: they account for the turbulent diffusion; the variance tensor plays the role of a diffusion tensor similar to a generalised eddy-viscosity matrix. Both the deformation rate and rotation-rate contribute to diffusion, unlike to the classical eddy-viscosity model in which fluid rotation-rate is assumed to be irrelevant in turbulent modelling (see also following section 3.2).

Turbulent compressibility: the continuity equation (11) suggests that the flow is turbulent-compressible; i.e. the unresolved turbulence induces a local fluid compression or expansion.

The variance tensor is the key parameter of the pseudo-stochastic model. It has the physical dimension of a dynamic viscosity $[m^2/s]$ and carries information on the intensity and the anisotropy of the SUS. As already mentioned, a_{ij} can be interpreted as a generalised eddy-viscosity parameter. Implicitly, this leads to the hypothesis that the SUS influences the resolved flow as an alteration of fluid viscosity, that is an empirical consideration largely accepted. The divergence of the variance tensor is hereafter named *turbulent advection* velocity:

$$u_{\mathrm{TA},i} = -\frac{1}{2}\frac{\partial a_{ij}}{\partial x_j}, \tag{12}$$

while the divergence of the turbulent advection velocity measured the *turbulent compressibility*:

$$\Phi_{\mathrm{TC}} = \frac{1}{2}\frac{\partial^2 a_{ij}}{\partial x_i \partial x_j}, \tag{13}$$

and it is directly proportional to the isotropic turbulent factor p_t appearing in the modified pressure. The numerical simulations reported later allow to gain additional insights regarding these two quantities, we refer to section 5.3 for the numerical analysis.

3.2 Comparison with LES eddy-viscosity models

The LES methodology consists in applying a spatial filter to velocity field, and then directly resolve the filtered velocity and model the sub-filter velocities. See Sagaut [42] and Piomelli [34] for an extended introduction on this subject. Practically, the computational grid acts as an implicit spatial filter on the governing equations, which generates an extra term τ_{ij} in the classical Navier-Stokes equations:

$$\begin{cases} \dfrac{\partial \overline{u}_i}{\partial t} + \overline{u}_j \dfrac{\partial \overline{u}_i}{\partial x_j} = -\dfrac{\partial \overline{p}}{\partial x_i} + \nu \dfrac{\partial^2 \overline{u}_i}{\partial x_j \partial x_j} - \dfrac{\partial \tau_{ij}}{\partial x_j}, \\ \dfrac{\partial \overline{u}_i}{\partial x_i} = 0, \end{cases} \tag{14}$$

where the sub-grid scale (SGS) tensor is $\tau_{ij} = \overline{u_i u_j} - \overline{u}_i \overline{u}_j$, and the straight over-bar denotes the spatial filter associated to the local cell width, computed as $\overline{\Delta} = (\Delta x \Delta y \Delta z)^{1/3}$. Adopting the eddy-viscosity assumption, the

anisotropic part of such tensor reads:

$$\tau_{ij}^R = \tau_{ij} - \frac{\tau_{kk}}{3}\delta_{ij} = -2\nu_{\text{SGS}}\overline{S}_{ij}, \tag{15}$$

where ν_{SGS} is the SGS viscosity parameter, which has to be specified by additional models (e.g. Smagorinsky model, Spalart-Allmaras, $k-\omega$, $k-\epsilon$). Equation (15) implies that: (a) the anisotropic Reynolds stress tensor is aligned with the mean strain-rate tensor; (b) the two are directly proportional through a single parameter, equal for all the six independent components of τ_{ij}^R.

The pseudo-stochastic model is equivalent to a constant eddy-viscosity model if the variance tensor is expressed by $a_{ij} = 2\nu_{\text{SUS}}\delta_{ij}$ where the SUS viscosity ν_{SUS} is constant. In this sense, the pseudo-stochastic model can be considered a generalisation of the eddy-viscosity model. The theoretical advantages of the former to the latter are pointed out:

1. The PSS does not rely on hypothesis (a). The effects of unresolved scales of motion are given by a_{ij}, without imposing any constrains on the directions along with the SUS acts on the resolved flow.
2. The PSS does not rely on hypothesis (b). The tensorial form of a_{ij} allows to reproduce the anisotropy of unresolved turbulence, i.e. different turbulent contributions along different directions.
3. The extra terms in PSS account for turbulent effects usually not considered in the classical models, namely turbulent advection and turbulent compressibility.

The eddy-viscosity models are quite reasonable for simple shear flows and it is largely applied in computational fluid dynamics. However, most of their shortcomings derive from the fact that hypotheses (a) and (b) are not generally satisfied; see Pope [35]. Efforts have been made to develop alternative models where the principal axis of τ_{ij}^R are not forced to be aligned with those of the mean strain tensor (e.g. the Reynolds-stress models), or where equation (15) is substituted by a non-linear viscosity models, in which the rotation strain-rate comes into play, see for example Bauer *et al.* [1]. In geophysical flow simulations, the strong grid anisotropy between horizontal and vertical directions is successfully handled using a directional eddy-viscosity, see Roman and Armenio [41].

It is worth mentioning that the eddy-viscosity parameter a_{ij} comes directly from the basic assumption of velocity decomposition in a smooth and a fast oscillating components (3), whereas it is introduced in LES equations through an *ad hoc* physical assumption.

4 Variance tensor model

In the LES framework, a popular model for ν_{SGS} in LES methodology is the the Smagorinsky model, first proposed by Smagorinsky [43] for simulation of environmental flows (see also Deardorff [7]). It is derived under the hypothesis

of local equilibrium between production and dissipation of turbulent kinetic energy, and reads:

$$\nu_{\mathrm{SGS}} = c_s^2 \overline{\Delta}^2 |\overline{S}|, \tag{16}$$

where $|\overline{S}|$ is the norm of the strain-rate tensor. The parameter c_s^2 is set constant and can be evaluated from experiments, direct numerical simulations or analytical considerations, e.g. see Lilly [23].

In order to perform a close comparison with the LES methodology, the variance tensor is modelled by a simple model analogous to the Smagorinsky model:

$$a_{ij} = c_m \Delta^2 |\overline{S}| \delta_{ij} \tag{17}$$

where Δ is the cell grid width and c_m is a model parameter. Hence, the variance tensor reduces to a diagonal matrix with equal elements because turbulence is assumed isotropic and homogeneous in all directions.

The relation with the classical Smagorinsky model is now highlighted. In LES, having applied the Smagorinsky model, the anisotropic Reynolds stress tensor reads:

$$-\frac{\partial \tau_{ij}^R}{\partial x_i} = \frac{\partial}{\partial x_i}\left(2 c_s^2 \Delta^2 |\overline{S}| S_{ij}\right) = S_{ij}\frac{\partial C_s |\overline{S}|}{\partial x_i} + \frac{C_s}{2}|\overline{S}|\frac{\partial^2 w_j}{\partial x_i \partial x_i}, \tag{18}$$

where $C_s = 2c_s^2\Delta^2$ denotes an auxiliary variable, c_s^2 is the Smagorinsky parameter and the velocity is divergence-free. In the PSS, the total turbulent model can be expressed by a single term, that gathers the dissipative and turbulent advective contributions. Applying formula (17) with $c_m = 2c_s^2$ and defining $C_m = c_m \Delta^2$, such a term becomes:

$$\frac{1}{2}\frac{\partial^2 a_{sk} w_i}{\partial x_s \partial x_k} = \underbrace{\left(S_{ij}\frac{\partial C_m |\overline{S}|}{\partial x_i} + \frac{C_m}{2}|\overline{S}|\frac{\partial^2 w_j}{\partial x_i \partial x_i}\right)}_{eddy-viscosity\ terms} + \underbrace{\Omega_{ij}\frac{\partial C_m |\overline{S}|}{\partial x_j}}_{rotational\ term} + \underbrace{\frac{w_i}{2}\frac{\partial^2 C_m |\overline{S}|}{\partial x_j \partial x_j}}_{strain-rate\ diff.}, \tag{19}$$

where the first two terms on the right-hand side have (formally) the same expression as (18), while the third and fourth term are additional contributions.

The PSS with isotropic constant model reduces to the LES Smagorinsky model under two approximations:

1. the rotation-rate does not contribute to turbulence effects on the mean flow, thus it is neglected;
2. the norm of strain-rate tensor is almost harmonic (Laplacian is close to zero), which makes the fourth term negligible.

Notice that the latter hypothesis implies that the continuity equation (6) turns into the classical solenoidal constrain. Therefore, the LES Smagorinsky model can be interpreted as a particular case of the PSS constant isotropic model.

Approximation (1) is valid if the turbulent energy is mainly concentrated in the region where the irrotational strain dominates vorticity. Exceptions on this behaviour have been found and have motivated the development of alternative

models, like the Wall Adaptive Local Eddy-viscosity (WALE) model of Nicoud and Ducros [30] or the structure function model of Métais and Lesieur [25]. Approximation (2) implies that the flow deformation rate can be represented by a linear function in each spatial point; thus it is a particularly regular function. This is equivalent to neglect the turbulent correction on advective velocity and continuity equation, hence the associated physical phenomena of turbophoresis and turbulent compressibility are not reproduced.

5 Numerical simulations

PSS and LES are compared on turbulence channel flow at $Re_\tau = 590$. The former adopts a constant isotropic model for variance tensor, the latter adopts a constant Smagorinsky model for sub-grid scale viscosity. The Direct Numerical Simulation (DNS) of Moser *et al.* [28] is taken as reference.

5.1 Case geometry and settings

The channel is composed by two horizontal and parallel walls between which a shear flow develops. The dimensions in stream-wise (x), vertical (y) and span-wise (z) directions are $2\pi\delta \times \delta \times \pi\delta$, respectively. The flow is driven by a constant pressure gradient $\frac{\partial p}{\partial x} = -\rho u_\tau/\delta$. The Reynolds number based on the friction velocity u_τ is defined as $Re_\tau = u_\tau\delta/\nu$. The spatial variables are made non-dimensional as $y^+ = yu_\tau/\nu$, the velocity as $u^+ = u/u_\tau$, time as $t^+ = tu_\tau/\nu$. The characteristic flow time is estimated as $t_0 = U_0/2\pi\delta$, where U_0 is the bulk velocity in stream-wise direction.

The computational domain is discretised by $96 \times 96 \times 96$ points. They are uniformly distributed in stream-wise and span-wise directions, leading to a cell width $\Delta x^+ < 40$ and $\Delta z^+ < 20$, respectively. In vertical direction, the grid is stretched in a way such that the first cell is within $y^+ = 1$ and with 9 cells in $y^+ \leq 11$; thus ensuring an accurate resolution of the boundary layer. The stretching is symmetric with respect to the channel centre plane $y = \delta$, and it is obtained with a double-side stretching function based on hyperbolic tangent:

$$y(\xi) = \frac{1}{2}\left(1 + \frac{\tanh(\lambda(\xi - 1/2))}{\tanh(\lambda/2)}\right), \tag{20}$$

where ξ is the vertical coordinate of uniform point distribution and the stretching factor is set to $\lambda = 5.25$.

Cyclic boundary conditions are set at the vertical boundaries, while velocity no-slip condition and pressure zero-gradient are imposed at the horizontal walls. All the cases are initialised with the instantaneous fields provided by a preliminary LES with constant Smagorinsky SGS model, that has reached the statistical steady state.

5.2 Algorithm and implementation

Simulations are performed taking advantage of the open-source software OpenFOAM v. 2.3.0. This is a C++ library for computational fluid dynamics and adopts the finite volume methods.

The LESs are carried out using the solver `pisoFoam` included in the standard software distribution. The implementation details on this basic solver can be found in the official OpenFOAM documentation and in the work of Jasak *et al.* [15]. The constant Smagorinsky SGS model is provided by OpenFOAM, and its correct implementation was checked.

Two PSSs are performed using the code `pseudoStochasticPisoFoam`, a home-made solver developed by the authors within the Fluminance research group at INRIA Rennes (France). The non-conservative form of pseudo-stochastic governing equations (5) are solved employing the Pressure-Implicit with Splitting of Operators (PISO) algorithm proposed by Issa *et al.* [14] and Oliveira & Issa [32].

Variables are discretised in space with a second-order central difference scheme, while time integration is performed using an implicit Euler backward scheme. Such a scheme employs the variables at the previous two time steps, leading to a second order accuracy. Globally, the numerical solvers are second-order accurate in time and space. The time advancement fulfils the Courant-Friedrichs-Lewy condition $Co < 0.5$. The Courant number is computed as $Co = \Delta t|v|/\delta x$, where: Δt is the time step, $|v|$ is the velocity magnitude through the cell, δx is the cell length. The model constants are chosen to be $c_s^2 = c_m/2 = 0.004225$, and for PSS $v = w^*$ while for LES $w^* = u$.

5.3 Results discussion

The simulations are run till the statistical steady state is reached, then they are re-run for an additional period of $12t_0$ where the statistics are collected. The quantities are averaged in time and in space along span-wise and stream-wise directions, and exploiting the domain symmetry in vertical direction. The angular brackets $\langle\psi\rangle$ denote the average in time and wall-parallel directions for a generic variable ψ.

First and second order statistics

The first and second order statistics of the velocity filed are analysed.

Figure 1 top-panel reports the mean non-dimensional stream-wise velocity along the wall coordinate. PSS and LES lead to similar profiles in the near-wall region ($y^+ < 30$), while the former exhibits slightly lower values in the log-law region ($y^+ > 30$). They underestimate the velocity magnitude at the centre channel and, as expected, both are not accurate in reproducing the boundary layer profile. This is a well known shortcoming of Smagorinsky model when c_s^2 is constant, and it is inherited by the constant isotropic model.

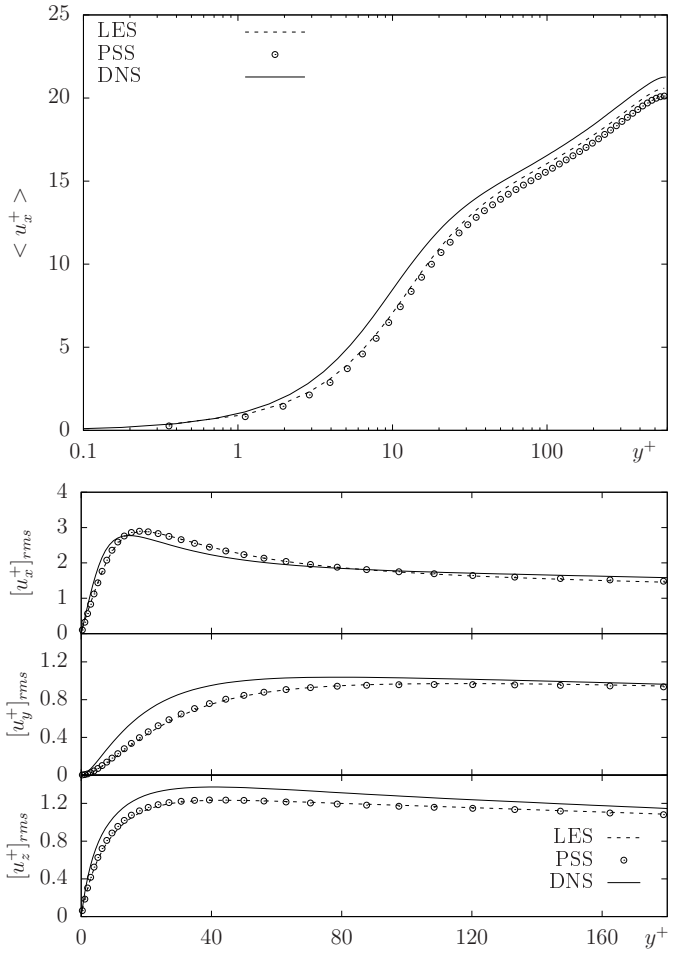

Fig. 1 First and second order statistics of velocity field versus non-dimensional vertical coordinate (wall coordinate). Top panel: non-dimensional mean stream-wise velocity. Bottom panel: non-dimension velocity root-mean square. Reference DNS by [28].

Figure 1 bottom-panel displays the velocity RMS components. If ψ is a generic variable, we denote $[\psi]_{rms} = \sqrt{\langle \psi'^2 \rangle}$ the root-mean square, where $\psi' = \psi - \langle \psi \rangle$ is the instantaneous fluctuation. Both PSS and LES collapse on the same profiles.

Because the isotropic model is very similar to the Smagorinsky model, an improvement of accuracy by the PSS is not expected. The interest of this validation is to prove that the pseudo-stochastic model is as accurate as the state-of-the-art LES methodologies, despite its derivation relies to a substantially different framework and its governing equations include several extra terms, which are analysed in the following sections.

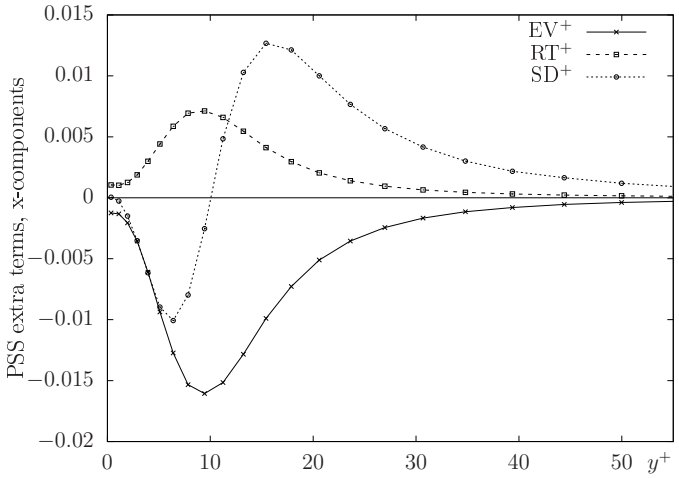

Fig. 2 Mean value of non-dimensional terms appearing in the pseudo-stochastic model with constant isotropic model, equation (19): component x along the wall-normal coordinate. EV, eddy-viscosity terms; RT, rotational term; SD, strain-rate diffusion.

Effects of the extra terms in PSS

The LES constant Smagorinsky model and the PSS constant isotropic model lead to similar governing equations, but the latter has some additional terms not present in the former: the eddy-viscosity terms (EV), the rotational term (RT) and the strain-rate diffusion (SD) defined in equation (19). The influence of such terms is checked.

Figure 2 shows the x-component of the above-mentioned terms (averaged) versus the wall coordinate. They are made non-dimensional by u_τ^3/ν. In LES, the term EV accounts for all sub-grid scale effects and represents a negative turbulent diffusion near the wall. In the PSS constant isotropic model, two other terms come into play: SD is negative in the region $y^+ < 10$, while it shows positive value at $y^+ > 10$; RT exhibits a positive contribution against the negative one of EV. The three terms become negligible in the log-law region; hence, the SUS model acts mainly at the near-wall region. The point $y^+ = 10$, located in the buffer layer, is of particular interest: approximately at this height, EV and RT reach the minimum and maximum (respectively), while SD changes sign. Globally, the RT and SD terms reduce the negative contribution of EV to the velocity equations in the buffer region, eventually producing a positive turbulent diffusion.

Turbulent advection and compressibility

Figure 3 presents the non-dimensional turbulent advection velocity $u^+_{\mathrm{TA}} = u_{\mathrm{TA}}/u_\tau$ and the turbulent compressibility $\Phi^+_{\mathrm{TC}} = \Phi_{\mathrm{TC}} u_\tau^2/\nu$ are scrutinised. The stream-wise component of u_{TA} is practically zero, as well as the span-wise component; thus they are not displayed. The vertical component profile reveals low

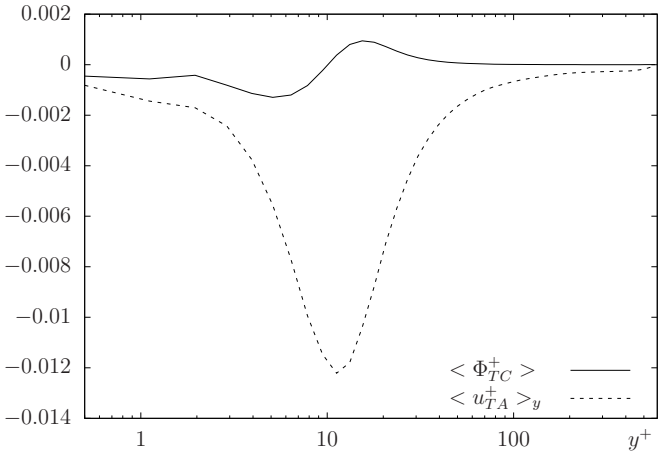

Fig. 3 Mean value of non-dimensional turbulent advenction (12) and compressibility (13) appearing in the pseudo-stochastic model with constant isotropic model: x-component along the wall coordinate.

negative values, with a climax at $y^+ \cong 10$. Quantitatively, the turbulent advection is not strong enough to produce remarkable results on the mean flow; however, it generates a weak vertical velocity w_y directed from the center to the wall of the channel (not reported). Hence, u_{TA} is qualified as a weak turbophoresis velocity: it advects the flow from the buffer region to the log-law region, i.e. in the direction of decreasing turbulence level (estimated by the velocity RMS intensity). The turbulent compressibility Φ_{TC} assumes negative values in the viscous sub-layer and positive values in the buffer layer. Elsewhere, it is practically zero. In light of equation (11), this behaviour is related to the presence of a turbulent fluid compression and expansion, respectively. Additional insight on this phenomenon is gained visualising the Φ_{TC} instantaneous values.

Figure 4 displays the Φ_{TC} negative (blue) and positive (orange) isosurfaces near the bottom wall, at an instantaneous flow configuration. They are organised in spots, confined in the near-wall region and elongated in the stream-wise direction. In accordance with the Φ_{TC} mean profile, the negative spots are closer to the wall ($y^+ < 10$), while the positive one are immediately above ($10 < y^+ < 20$). The shape and the location of the isosurfaces suggest a correlation with the *streaks* structures that characterises turbulent wall flows. The streaks are generated in a region of low velocity, very close to the wall, approximately at $y^+ \simeq 5$. They are elongated in the stream-wise direction, with a characteristic length of $\Delta x^+ \cong 1000$ and a span-wise period of $\Delta z^+ \cong 100$. This estimation can vary with respect to the wall distance, see Smith & Metzler [44]. Despite their widespread presence, there is no clear consensus on the streak formation mechanism and multiple theories have been proposed in literature, see Chernyshenko & Baig [6]. The Φ_{TC} isosurfaces have, overall, the

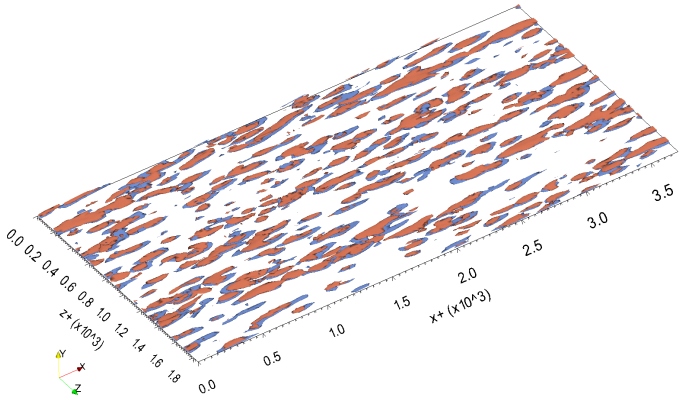

Fig. 4 Positive and negative isosurfaces of Φ_{TC} near the bottom wall at an instantaneous flow configuration. Orange: isosurface at $\Phi^+_{\text{TC}} = 3.5/times10^-4$. Blue: isosurface at $\Phi^+_{\text{TC}} = -3.5/times10^-4$.

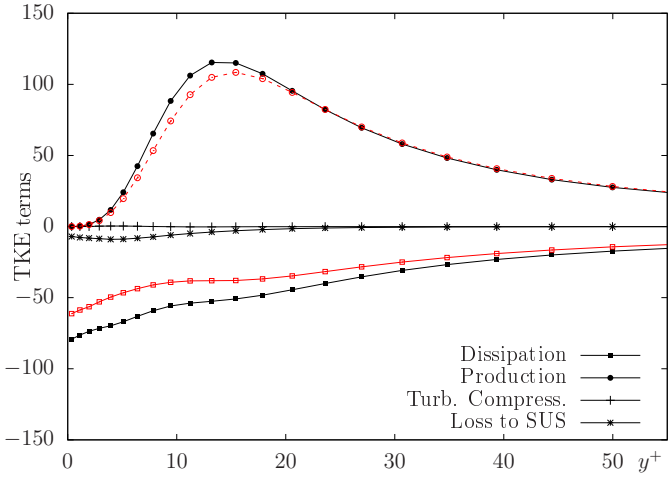

Fig. 5 Selected contributions to the pseudo-stochastic TKE budget versus wall-normal coordinate. The TKE terms are labelled as in equation (8). Results of three simulations are displayed: PSS with constant isotropic model, black lines with solid symbols; LES with constant Smagorinsky model, red lines with empty symbols.

same stream-wise extension and span-wise period. Also, the negative spots are located at the same height at which steaks are triggered. Therefore, these two structures appears to be related.

Resolved turbulent kinetic budget

The pseudo-stochastic TKE budget (8) is finally scrutinised for PSS and LES simulations

Figure 5 shows selected terms of the TKE budget. Production and dissipation profiles are similar for PSS and LES, but the former appears to be more effective in energy dissipation in near-wall region and has a higher production of TKE in the range $5 < y^+ < 20$. In the PSS, the turbulent compression term is almost zero and does not contribute to the budget; while the loss due to SUS presents slightly negative values mainly localised in the viscous layer. Hence, it contributes to global energy dissipation.

6 Conclusions

The pseudo-stochastic simulation (PSS) methodology introduced by Mémin [24] is analysed theoretically and numerically, through a direct comparison with the classical large-eddy simulations (LES) approach. The PSS model is based on an innovative decomposition of the fluid-particle trajectory in a drift displacement and a stochastic perturbation. The former reproduces the mean flow, the later accounts for the turbulent perturbations which are modeled as a Brownian motion. Imposing such a decomposition, together with a regularity assumption on the drift velocity, a set of deterministic and stochastic equations of motion are derived using stochastic calculus; then, the pseudo-stochastic equations are obtained by neglecting the solution of stochastic equations and closing the system by physical assumptions. The result is a new set of governing equations which includes extra terms deriving from the stochastic modeling of turbulence. The PSS model is found to be a generalisation of the classical Navier-Stokes equations, and reproduces phenomena usually not considered: turbophoresis and turbulent compressibility.

The PSS of turbulent channel flow at $Re_\tau = 590$ is performed, together with the LES with constant Smagorinsky sub-grid scale model. For a better comparison, a closure model analogous to the Smagorinsky one is used for the PSS. However, it is shown that this last does not rely on the eddy-viscosity hypotheses, hence it is not affected by its shortcomings. The PSS does not show improvement in first and second order statistics, possibly because of the simple expression of a_{ij}, but reproduces additional features: a weak turbophoresis is detected in the buffer region, while a turbulent compression and expansion is identified in the viscous and buffer layer (respectively). This quantity appears to be related to the streaks, turbulent structures appearing near the wall region.

Finally, the pseudo-stochastic model is a generalisation of the LES eddy-viscosity model and describes a richer physics. Overall, it represents a promising approach for simulation of turbulent flows: the mathematical analysis here reported gives a clear physical interpretation of the model, supported by numerical results.

A . Formal derivation of stochastic model

The mathematical conditions under which this derivation is consistent are reported in [9,26,27]. An introduction to the mathematical framework in which the present model is developed can be found in Øksendal [31] and Kunita [18].

A.1 Trajectory and stochastic velocity definitions

As already mentioned, expression (1) has to be understood in an integral sense:

$$X_t^i = X_0^i + \int_0^t w_i(X_s, s)ds + \int_0^t d\eta_s^i(X_s), \tag{21}$$

where the Itō stochastic integral is used to integrate the random process. The process $X_t^i(x_0)$ is a semimartingale defined for each spatial point $x_0 \in \Omega$ and time $t \in T \subseteq \mathbb{R}^+$ in an appropriate probability space.

The stochastic velocity in equation (3) is a symbolic expression that is defined as a weak derivative of the random displacement:

$$\int h(t)\dot{\eta}_t^i(x)dt = \int h'(t)\eta_t^i(x)dt, \tag{22}$$

for each h test function; see also [31].

A.2 The stochastic Reynolds transport theorem

Being the velocity field a stochastic process, the governing equations of fluid dynamics cannot be recovered using deterministic calculus, ref. [24,27]. In this concern, the key point is to give an expression of the *Reynolds transport theorem* (RTT) for stochastic quantities. Subsequently, the stochastic Navier-Stokes equations are found imposing conservation of mass and momentum.

Theorem 1 (Stochastic RTT) *Let us consider a physical quantity $q(x,t)$ within a material volume $V(t) \subset \mathbb{R}^3$, transported by a stochastic flow of the form (1) and such that it can be written as a semimartingale of the type:*

$$q(x,t) = q(x,0) + \int_0^t g(x,s)ds + \int_0^t \int_\Omega f_k(x,y,s)dB_s^k(y)dyds, \tag{23}$$

where g, f are processes of bounded-variation and the Itō integral are employed. If the following properties holds:

1. *symmetric diffusion tensor: $\sigma_{ij} = \sigma_{ji}$,*
2. *solenoidal diffusion tensor: $\frac{\partial}{\partial x_i}\sigma_{ij}(x,y,t) = 0$ for all j,*
3. *conserved quantity: $dq(X_t,t) = 0$,*

then the stochastic RTT has an explicit differential form that reads:

$$d\int_{V(t)} q(x,t)dx = \int_{V(t)} \left[\partial_t q + \frac{\partial(qw_i)}{\partial x_i}dt - \frac{1}{2}\frac{\partial^2(qa_{ij})}{\partial x_i \partial x_j}dt + \frac{\partial q}{\partial x_i}d\eta_t^i\right]dx, \tag{24}$$

where ∂_t is the differential with respect to the second variable, and d denotes the total time increment at a fixed spatial point.

Assumption (1) greatly simplifies the computation and can be justified *a posteriori*: it implies that the variance tensor a_{ij} is symmetric, a desirable properties in light of its physical interpretation (see section 3.1). Therefore, this assumption is considered reasonable in the fluid dynamics context; however it is not mandatory, see [37]. Hypothesis (2) can be removed, but the stochastic RTT expression assumes a more complex formulation. It is found that this constrain is naturally satisfied by fluids where density is constant in space (see section A.3), thus formula (24) is directly applied when the flow is incompressible or when the Boussinesq approximation is applied. On the contrary, an explicit formula has not been derived for a generic non-conserved quantity; hence hypothesis (3) is essential.

Notice that equation (24) reduces to the classical RTT when the stochastic contribution in equation (1) is suppressed. This happens e.g. when $\sigma_{ij} = 0$ and, consequently, the martingale η_t^i as well as the variance tensor are identically zero.

A concise derivation of the stochastic RTT is now presented. A generic random process $\phi(x,t)$ is expressed hereafter as a semimartingale of the form:

$$\phi(x,t) = \phi(x,0) + \int_0^t g(x,s)ds + \int_0^t \int_\Omega f_k(x,y,s)dB_s^k(y)dyds, \tag{25}$$

where g, f are processes of bounded-variation and the Itō integral are used.

Proposition 1 (Differential of transported process) *Let us consider ϕ a semimartingale of the type (25), sufficiently regular in space (bounded spatial gradient, two times derivable). If it is transported by a flow of the form (21); then, the time total-differential of ϕ is expressed by:*

$$d\phi(X_t,t) = \partial_t\phi + \frac{\partial\phi}{\partial x_i}dX_t^i + \frac{1}{2}a_{ij}(X_t,t)\frac{\partial^2\phi}{\partial x_i\partial x_j}dt + \int_\Omega \sigma_{ij}(X_t,y,t)\frac{\partial}{\partial x_i}f_j(X_t,y,t)dydt, \tag{26}$$

where ∂_t is the time partial-differential (i.e. with respect to second variable), and a_{ij} is the variance tensor defined by equation (4).

Proof: The Itō -Wentzell formula is used to differentiate (in time) the transported process $\phi(X_t,t)$, corresponding to a composition of two processes. It reads:

$$d\phi(X_t,t) = \partial_t\phi + \frac{\partial\phi}{\partial x_i}dX_t^i + \frac{1}{2}d\left\langle X^i, X^j\right\rangle_t \frac{\partial^2\phi}{\partial x_i\partial x_j} + d\left\langle \frac{\partial\phi}{\partial x_i}, X^i\right\rangle_t, \tag{27}$$

where the angular brackets denote the quadratic variation operation; e.g. see Le Gall [19] for an extended presentation. The following properties of the quadratic variation are recalled:

1. is symmetric and bilinear;
2. if g is a process of bounded-variation: $\left\langle g, B^k\right\rangle_t = 0$
3. if f is deterministic function: $\left\langle fB^i, B^j\right\rangle_t = f\left\langle B^i, B^j\right\rangle_t$
4. singularity: $d\left\langle B^i(y), B^j(z)\right\rangle_t = \delta(y-z)\delta_{ij}dt$

where B_t is a cylindrical Wiener process, $\delta(x)$ is the Dirac function and δ_{ij} is the Kronecker symbol. Using these properties, the third and fourth terms in equation (27) are written explicitly. The third term is directly computed:

$$d\left\langle X^i, X^j\right\rangle_t = \int_\Omega \sigma_{ik}(X_t,y,t)\sigma_{jk}(X_t,y,t)dydt = a_{ij}(X_t,t)dt. \tag{28}$$

In the fourth term, the gradient of ϕ is obtained differentiating equation (25):

$$\frac{\partial}{\partial x_i}\phi(X_t,t) = \frac{\partial\phi_0}{\partial x_i} + \int_0^t \frac{\partial}{\partial x_i}g(X_s,s)ds + \int_0^t\int_\Omega \frac{\partial}{\partial x_i}f_k(X_s,y,s)\ dB_s^k(y)dyds, \tag{29}$$

then, the last term in (27) is rewritten as:

$$d\left\langle \frac{\partial\phi}{\partial x_i}, X^i\right\rangle_t = \int_\Omega \sigma_{ij}(X_t,y,t)\frac{\partial}{\partial x_i}f_j(X_t,y,t)dydt. \tag{30}$$

Substituting formula (28) and (29) in equation (27), expression (26) is recovered. □

Proposition 2 (Differential of transported and conserved process) *Let us consider a stochastic process ϕ of the type (25). If such a process is transported by a stochastic flow (21) and is conserved, i.e. $d\phi(X_t,t)=0$, then:*

$$\partial_t\phi(X_t,t) = -\frac{\partial\phi}{\partial x_i}w_i dt + \frac{1}{2}a_{ij}\frac{\partial^2\phi}{\partial x_i\partial x_j}dt + \int_\Omega \frac{\partial\phi}{\partial x_k}\frac{\partial\sigma_{kj}}{\partial x_i}\sigma_{ij}dydt - \int_\Omega \frac{\partial\phi}{\partial x_i}\sigma_{ik}dB_t^k dy. \tag{31}$$

This formula expresses the time variation along a fluid-particle trajectory.

Proof: If $\phi(X_t,t)$ is conserved, then equation (26) can be re-arranged as follows:

$$\begin{aligned}\partial_t\phi(X_t,t) = &-\frac{\partial\phi}{\partial x_i}w_i dt - \int_\Omega \frac{\partial\phi}{\partial x_i}\sigma_{ik}(X_t,y,t)dB_t^k(y)dy - \\ &- \frac{1}{2}a_{ij}\frac{\partial^2\phi}{\partial x_i\partial x_j}dt - \int_\Omega \sigma_{ij}(X_t,y,t)\frac{\partial}{\partial x_i}f_j(X_t,y,t)dydt.\end{aligned} \tag{32}$$

An expression of $\partial_t\phi$ is obtained also from (25), and is compared with formula (32). Exploiting the unique decomposition of the semimartingales, one obtains:

$$g(X_t,t) = -\frac{\partial\phi}{\partial x_i}w_i - \frac{1}{2}a_{ij}\frac{\partial^2\phi}{\partial x_i\partial x_j} - \int_\Omega \sigma_{ij}(X_t,y,t)\frac{\partial}{\partial x_i}f_j(X_t,y,t)dy, \tag{33}$$

and the following implicit formula for f:

$$\int_\Omega \left[f_k(X_t,y,t) + \frac{\partial\phi(X_t,t)}{\partial x_i}\sigma_{ik}(X_t,y,t)\right]dB_t^k(y)dy = 0. \tag{34}$$

This latter holds for every Brownian motion dB_t^k, thus:

$$f_k(X_t,y,t) = -\frac{\partial\phi(X_t,t)}{\partial x_i}\sigma_{ik}(X_t,y,t). \tag{35}$$

Substituting formula (35) in equation (32) the final expression (31) is obtained. □

Notice that a general form of a conserved semimartingale can be found by substituting equation (33) and (35) in formula (25).

Translating equation (31) from Lagrangian to Eulerian coordinates and rearranging the second and third terms in the left-hand side, one obtains the expression of the material derivative (in differential form) within the stochastic framework.

Proposition 3 (Stochastic transport operator) *If ϕ is a stochastic process of the type (25), transported by a stochastic flow (21) and conserved, then the stochastic material derivative in differential form is:*

$$\begin{aligned}D\phi(x,t) = &\partial_t\phi + (w_i dt + d\eta_t^i)\frac{\partial\phi}{\partial x_i} - \frac{1}{2}\frac{\partial}{\partial x_i}\left(a_{ij}\frac{\partial\phi}{\partial x_j}\right)dt \\ &- \left(\frac{1}{2}\frac{\partial a_{ij}}{\partial x_i} - \int_\Omega \sigma_{kj}\frac{\partial\sigma_{ij}}{\partial x_i}dy\right)\frac{\partial\phi}{\partial x_j}dt,\end{aligned} \tag{36}$$

which is reported in [37] as the stochastic transport operator for a conserved quantity.

The derivation of Stochastic RTT is now summarised. Let us consider a generic physical quantity, mathematically expressed by a stochastic scalar process $q(x,t)$ that satisfies the hypotheses of Stochastic RTT. The solution of transport equation is found in the space of weak solutions.

Proof (Stochastic RTT): Consider a control volume $V(t)$ and a test function $\varphi(x,t)$ in the space domain Ω such that: it has compact support on $V(t)$, it is conserved and satisfies (25). Then, the weak transport equation for q reads:

$$d\int_{V(t)} q(x,t)\varphi(x,t)dx = \int_{\Omega}\left[\varphi\partial_t q + q\partial_t\varphi + d\left\langle q,\varphi\right\rangle_t\right]dx, \tag{37}$$

applying the Itō integration by part and passing to the integral on Ω because φ has compact support on V. The last term on the right-hand side needs to be explicited. An expression of q and φ is given by the semimartingale decomposition (25):

$$\varphi = \varphi(x,0) + \int_0^t g(x,s)ds + \int_0^t\int_{\Omega} f_j(x,y,s)dB_s^j dy, \tag{38}$$

$$q = q(x,0) + \int_0^t h(x,s)ds + \int_0^t\int_{\Omega} \kappa_j(x,y,s)dB_s^j dy, \tag{39}$$

where explicit formulae for g,h,f,κ are given, see proof of Proposition 2. Using these expressions to compute the quadratic variation, we get:

$$d\left\langle q,\varphi\right\rangle_t = d\int_0^t\left\langle\int_{\Omega}\kappa_i dB^i dy, \int_{\Omega} f_j dB^j dz\right\rangle_t = \frac{\partial q}{\partial x_k}\frac{\partial\varphi}{\partial x_\ell}a_{k\ell}dt, \tag{40}$$

The same expressions are differentiated to express $\partial_t q(x,t)$ and $\partial_t\varphi(x,t)$, that are substituted in the transport equation (37) together with formula (40). Subsequently, φ is used to compute the weak derivative and gathered; the final equation reads:

$$\begin{aligned} d\int_{\Omega} q(x,t)\varphi(x,t)dx = \int_{\Omega}\varphi\Bigg[&\partial_t q + \frac{\partial q w_i}{\partial x_i}dt + \frac{1}{2}\frac{\partial^2}{\partial x_i\partial x_j}\left(qa_{ij}\right)dt - \\ &- \frac{\partial}{\partial x_k}\int_{\Omega} q\frac{\partial\sigma_{kj}}{\partial x_i}\sigma_{ij}dydt + \frac{\partial}{\partial x_i}\left(qd\eta_t^i\right) - \frac{\partial}{\partial x_\ell}\left(\frac{\partial q}{\partial x_k}a_{k\ell}\right)dt\Bigg]dx. \end{aligned} \tag{41}$$

Equation (41) is valid for every test function φ with compact support in $V(t)$, thus:

$$\begin{aligned} d\int_V q(x,t)dx = \int_V\Bigg[&\partial_t q + \frac{\partial q w_i}{\partial x_i}dt + \frac{\partial}{\partial x_i}\left(qd\eta_t^i\right) + \frac{1}{2}q\left\|\frac{\partial\sigma}{\partial x}\right\|^2 dt \\ &- \frac{1}{2}\int_{\Omega}\left(q\frac{\partial\sigma_{ik}}{\partial x_j}\frac{\partial\sigma_{kj}}{\partial x_i} + \frac{\partial^2 q}{\partial x_i\partial x_j}\sigma_{ik}\sigma_{kj} + 2\sigma_{ij}\frac{\partial q}{\partial x_k}\frac{\partial\sigma_{kj}}{\partial x_i}\right)dydt\Bigg]dx, \end{aligned} \tag{42}$$

where the terms are rearranged and the definition of variance tensor is used to simplify some terms. Equation (42) is the general form of Stochastic RTT, that is quite complex and eventually difficult to handle. One can notice that under the additional hypothesis that the random term is solenoidal in space, i.e.

$$\frac{\partial}{\partial x_i}d\eta_t^i(x) = 0 \quad\Leftrightarrow\quad \frac{\partial}{\partial x_i}\sigma_{ik}(x,y,t) \equiv 0, \tag{43}$$

where the if and only if statement holds because the Brownian motion is arbitrarily chosen, the equation (42) simplifies to:

$$d\int_V q(x,t)\,dx = \int_V\left[\partial_t q + \frac{\partial\left(qw_i\right)}{\partial x_i}dt - \frac{1}{2}\frac{\partial^2\left(qa_{ij}\right)}{\partial x_i\partial x_j}dt + \frac{\partial\left(qd\eta_t^i\right)}{\partial x_i}\right]dx, \tag{44}$$

that is the final form of Stochastic RTT. □

In the following section, it is shown that the assumption of a solenoidal random turbulence field is satisfied by incompressible fluids, thus the simpler equation (44) can be used to derived the equation of motion.

It is worth noticing that the Stochastic RTT can be applied to all functions of the form (25); specifically, to all process of bounded-variations that are a particular case of semimartingale where the martingale term is zero.

A.3 Derivation of Stochastic Navier-Stokes equations

The derivation of governing equations for fluid flows is performed with a similar strategy as in the classical framework, e.g. see [17].

Conservation of mass

If $\rho(x,t)$ is the mass density, then the conservation of mass is:

$$d\int_{V(t)}\rho dx = \int_{V(t)}\Bigg[\partial_t\rho + \frac{\partial \rho w_i}{\partial x_i}dt + \frac{\partial}{\partial x_i}\left(\rho d\eta_t^i\right) + \frac{1}{2}\rho\left\|\frac{\partial\sigma}{\partial x}\right\|^2 dt \tag{45}$$

$$-\frac{1}{2}\int_\Omega\left(\rho\frac{\partial\sigma_{ik}}{\partial x_j}\frac{\partial\sigma_{kj}}{\partial x_i} + \frac{\partial^2\rho}{\partial x_i\partial x_j}\sigma_{ik}\sigma_{kj} + 2\sigma_{ij}\frac{\partial\rho}{\partial x_k}\frac{\partial\sigma_{kj}}{\partial x_i}\right)dydt\Bigg]dx = 0, \tag{46}$$

where the general form of Stochastic RTT (42) is used here. For an incompressible fluid, density is constant $\rho(x,t) = \rho$ and the mass conservation equation simplifies accordingly. The integral is then removed exploiting the arbitrariness of control volume:

$$\frac{\partial w_i}{\partial x_i}dt + \frac{\partial}{\partial x_i}d\eta_t^i + \frac{1}{2}\left\|\frac{\partial\sigma}{\partial x}\right\|^2 dt - \frac{1}{2}\int_\Omega\frac{\partial\sigma_{ik}}{\partial x_j}\frac{\partial\sigma_{kj}}{\partial x_i}\,dydt = 0. \tag{47}$$

Separating the processes of bounded-variation and the martingales, the following system is recovered:

$$\left(\frac{\partial w_i}{\partial x_i} + \frac{1}{2}\left\|\frac{\partial\sigma}{\partial x}\right\|^2 - \frac{1}{2}\int_\Omega\frac{\partial\sigma_{ik}}{\partial x_j}\frac{\partial\sigma_{kj}}{\partial x_i}dy\right)dt = 0, \quad \frac{\partial}{\partial x_i}d\eta_t^i = 0. \tag{48}$$

Equation (48) shows that for an incompressible fluid the Brownian term is solenoidal; thus, the use of the simplified expression Stochastic RTT (44) is *a posteriori* justified for incompressible fluids. Using the solenoidal constraint, equations (48) leads to the system:

$$\frac{\partial}{\partial x_i}\left(w_i - \frac{1}{2}\frac{\partial}{\partial x_j}a_{ij}\right) = 0, \quad \frac{\partial}{\partial x_i}\sigma_{ik} = 0, \tag{49}$$

which expresses the conservation of mass.

Conservation of momentum

Two derivations are proposed, they are named Lagrangian and Eulerian for convenience of notation. The former is based on the work of [27], the latter on that one of [24].

- Lagrangian: The second Newton's law is:

$$\frac{d}{dt}\rho U_i(X_t,t) = F_i(X_t,t), \tag{50}$$

where F_i are the forces acting on a fluid-particle. If I_i if the time integral of the forces (the *impulse*), equation (50) is re-written in a differential form as $d\rho U_i = dI_i$. It is expressed in a weak form as:

$$\rho\int h\; dU_i(X_t,t) = \int h\; dI_i(X_t,t), \tag{51}$$

where h are test functions and ρ is constant. The left-hand side is:

$$\rho\int h\; dU_i(X_t,t) = \rho\int h\; dw_i(X_t,t) - \rho\int h' d\eta_t^i, \tag{52}$$

then, the right-hand side of equation (51) must have the same structure, see [27]. Hence, the impulse divides into two contributions and equation (51) becomes:

$$\rho \int h\ dw_i(X_t,t) - \rho \int h' d\eta_t^i = \int h\ d\mathcal{J}_i - \int h' d\lambda_t^t. \tag{53}$$

Matching similar terms, we arrived at the following relations:

$$\rho dw_i = d\mathcal{J}_i, \quad d\eta_t^i = d\lambda_t^i. \tag{54}$$

Equations (54)-first is exploited to obtain the governing equation of motion, while (54)-second states that the forces balance the contribution of random velocities. In Eulerial framework, this latter reads:

$$\rho D w_i(x,t) = d\mathcal{J}_i(x,t), \tag{55}$$

Applying the stochastic transport operator (36) with the solenoidal constrain (49), one gets:

$$Dw_i = \partial_t w_i + (w_j - \frac{1}{2}\frac{\partial a_{kj}}{\partial x_k})\frac{\partial w_i}{\partial x_j}dt - \frac{1}{2}\frac{\partial}{\partial x_k}\left(a_{jk}\frac{\partial w_i}{\partial x_j}\right)dt + d\eta_t^j \frac{\partial w_i}{\partial x_j}, \tag{56}$$

while the impulse is determined by a physical analysis of the forces acting on the system, as in the classical derivation:

$$d\mathcal{J}_i = -\frac{\partial}{\partial x_i}(pdt - d\xi_t) + \mu\frac{\partial^2}{\partial x_j \partial x_j}\left(dX_t^i\right) + \frac{\mu}{3}\frac{\partial}{\partial x_i}\frac{\partial}{\partial x_\ell}\left(dX_t^\ell\right) \tag{57}$$

$$= \left[-\frac{\partial p}{\partial x_i} + \mu\frac{\partial^2 w_i}{\partial x_j \partial x_j} + \frac{\mu}{3}\frac{\partial^2 w_\ell}{\partial x_i \partial x_\ell}\right]dt - \frac{\partial(d\xi_t)}{\partial x_i} + \mu\frac{\partial^2\left(d\eta_t^i\right)}{\partial x_j \partial x_j} + \frac{\mu}{3}\frac{\partial^2\left(d\eta_t^\ell\right)}{\partial x_i \partial x_\ell}, \tag{58}$$

with μ is the fluid viscosity, and pressure is written in a semimartingale form (25) where $d\xi_t(x) = \int_\Omega \vartheta_i(x,y,t)dB_t^i(y)dy$ denotes the martingale contribution to pressure. Imposing the equality (55) and using the unique decomposition of semimartingale, the governing equations (63) are recovered.

• Eulerian: Once again, the momentum conservation is formulated in differential form. If $\mathcal{J}_i(x,t)$ is the impulse of total forces per volume, the second law of mechanics reads:

$$d\int_{V(t)} \rho U_i(x,t)dx = \int_{V(t)} d\mathcal{J}_i(x,t)dx. \tag{59}$$

The Stochastic RTT is applied to the left-hand side in order to get:

$$d\int_{V(t)} \rho U_i\, dx = \int_{V(t)} \rho\Bigg[\partial_t w_i + \frac{\partial}{\partial x_j}(w_i w_j)dt - \frac{1}{2}\frac{\partial^2}{\partial x_s \partial x_k}(w_i a_{sk})\,dt + \\ + \frac{\partial}{\partial x_j}\left(w_i d\eta_t^j\right)\Bigg]dx + d\int_{V(t)} \rho\ \dot{\eta}_t^i dx, \tag{60}$$

where the velocity decomposition (3) is employed. The impulse acting on $V(t)$ is expressed by (58). Then, imposing equality (59) and separating the processes of bounded-variation to the martingales, one obtains:

$$\partial_t w_i + \frac{\partial w_i w_j}{\partial x_j}dt - \frac{1}{2}\frac{\partial^2(w_i a_{sk})}{\partial x_s \partial x_k}dt = -\frac{\partial p}{\partial x_i}dt + \nu\frac{\partial^2 w_i}{\partial x_j \partial x_j}dt + \frac{\nu}{3}\frac{\partial}{\partial x_i}\frac{\partial w_\ell}{\partial x_\ell}dt \tag{61}$$

with $\nu = \mu/\rho$ is the dynamic viscosity, and

$$d\int_{V(t)} \dot{\eta}_t^i dx = \int_{V(t)} \left[-\frac{\partial}{\partial x_i}d\xi_t + \nu\frac{\partial^2}{\partial x_j \partial x_j}d\eta_t^i - d\eta_t^j\frac{\partial w_i}{\partial x_j}\right]dx \tag{62}$$

where the conservation of mass constrain (49) is applied to simplify the formula. Notice that the expected value of noise is zero because the random displacement is uncorrelated in time. Then, the integral at the right-hand side can be interpreted as a spatial empirical mean of zero-mean random process, and have to be null. With this simplification, the system (63) of fluid dynamics equations is obtained.

Finally, the stochastic model for an incompressible (Newtonian) fluid reads:

$$\begin{cases} \dfrac{\partial w_i}{\partial t} + \dfrac{\partial (w_j w_i)}{\partial x_j} = -\dfrac{\partial p}{\partial x_i} + \nu \dfrac{\partial^2 w_i}{\partial x_j \partial x_j} + \dfrac{\nu}{3} \dfrac{\partial}{\partial x_i} \dfrac{\partial w_\ell}{\partial x_\ell} + \dfrac{1}{2} \dfrac{\partial^2 \left(a_{sk} w_i\right)}{\partial x_s \partial x_k} \\ \dfrac{\partial}{\partial x_i} \left(w_i - \dfrac{1}{2} \dfrac{\partial}{\partial x_j} a_{ij} \right) = 0 \\ \dfrac{1}{\rho} \dfrac{\partial}{\partial x_i} d\xi_t = \nu \dfrac{\partial^2}{\partial x_j \partial x_j} d\eta_t^i - d\eta_t^j \dfrac{\partial w_i}{\partial x_j} \\ \dfrac{\partial}{\partial x_i} d\eta_t^i = 0 \end{cases} \tag{63}$$

The system is composed by two coupled sets of deterministic and stochastic non-linear partial differential equations, in the unknowns w_i and σ_{ij}. The pseudo-stochastic model is obtained by avoiding the resolution of the last two stochastic equations, and closing the system by providing an expression a_{ij} through physical assumptions.

Let us also outline that the system (63) has been obtained under the assumption that the drift velocity is of bounded variation. Removing this assumption, the separation of the regular and the stochastic terms cannot be performed anymore. Hence, one obtains a fully stochastic Nevier-Stokes composed by stochastic partial differential equations. For geophysical flows (for isochoric flows in general), the continuity equations is also stochastic; see [37].

References

1. Bauer, W., Haag, O., Hennecke, D.: Accuracy and robustness of nonlinear eddy viscosity models. International Journal of Heat and Fluid Flow **21**(3), 312–319 (2000). DOI doi.org/10.1016/S0142-727X(00)00015-1
2. Brzeźniak, Z., Capiński, M., Flandoli, F.: Stochastic partial differential equations and turbulence. Mathematical Models and Methods in Applied Sciences **1**(01), 41–59 (1991)
3. Chandramouli, P., Heitz, D., Laizet, S., Mémin, E.: Coarse large-eddy simulations in a transitional wake flow with flow models under location uncertainty. Computers and Fluids **168**, 170 – 189 (2018). DOI doi.org/10.1016/j.compfluid.2018.04.001
4. Chapron, B., Drian, P., Mémin, E., Resseguier, V.: Largescale flows under location uncertainty: a consistent stochastic framework. Quarterly Journal of the Royal Meteorological Society **144**(710), 251–260 (2017). DOI 10.1002/qj.3198
5. Chasnov, J.R.: Simulation of the kolmogorov inertial subrange using an improved subgrid model. Physics of Fluids A: Fluid Dynamics **3**(1), 188–200 (1991). DOI 10.1063/1.857878
6. Chernyshenko, S.I., Baig, M.F.: The mechanism of streak formation in near-wall turbulence. Journal of Fluid Mechanics **544**, 99–131 (2005). DOI 10.1017/S0022112005006506
7. Deardorff, J.W.: A numerical study of three-dimensional turbulent channel flow at large reynolds numbers. Journal of Fluid Mechanics **41**(2), 453480 (1970). DOI 10.1017/S0022112070000691
8. Durbin, P.A., Speziale, C.G.: Realizability of second-moment closure via stochastic analysis. Journal of Fluid Mechanics **280**, 395–407 (1994). DOI 10.1017/S0022112094002983
9. Flandoli, F.: An Introduction to 3D Stochastic Fluid Dynamics, pp. 51–150. Springer Berlin Heidelberg, Berlin, Heidelberg (2008). DOI 10.1007/978-3-540-78493-7_2
10. Flandoli, F.: The interaction between noise and transport mechanisms in pdes. Milan Journal of Mathematics **79**(2), 543–560 (2011). DOI 10.1007/s00032-011-0164-5

11. Frederiksen, J.S.., O'Kane, T.J., Zidikheri, M.J.: Subgrid modelling for geophysical flows. Philosophical Transaction of Royal Society A **371**(1982) (2013)
12. Harouna, S.K., Mémin, E.: Stochastic representation of the reynolds transport theorem: Revisiting large-scale modeling. Computers and Fluids **156**, 456 – 469 (2017)
13. Holm, D.D.: Variational principles for stochastic fluid dynamics. Proceedings of the Royal Society of London A: Mathematical, Physical and Engineering Sciences **471**(2176) (2015). DOI 10.1098/rspa.2014.0963
14. Issa, R.I., Gosman, A.D., Watkins, A.P.: The computation of compressible and incompressible recirculating flows by a non-iterative implicit scheme. J. Computational Physics **62**, 66 (1986)
15. Jasak, H., Weller, H., Gosman, A.: High resolution NVD differencing scheme for arbitrarily unstructured meshes. Int. J. Numer. Meth. Fluids **31**, 431–449 (1999)
16. Kraichnan, R.H.: Dynamics of nonlinear stochastic systems. Journal of Mathematical Physics **2**(1), 124–148 (1961). DOI 10.1063/1.1724206
17. Kundu, P., Cohen, I.M.: Fluid Mechanics, third edn. Elsevier Academic Press (2004)
18. Kunita, H.: Stochastic Flows and Stochastic Differential Equations. Cambridge University Press (1997)
19. Le Gall, J.F.: Brownian Motion, Martingales, and Stochastic Calculus. Springer International Publishing (2016). DOI doi.org/10.1007/978-3-319-31089-3
20. Leith, C.E.: Stochastic backscatter in a subgridscale model: Plane shear mixing layer. Physics of Fluids A: Fluid Dynamics **2**(3), 297–299 (1990). DOI 10.1063/1.857779
21. Lesieur, M.: Turbulence in Fluids, *Fluid Mechanics and Its Applications*, vol. 84. Springer Netherlands (2008). DOI 10.1007/978-1-4020-6435-7
22. Leslie, D.C.: Developments in the theory of turbulence. Oxford, Clarendon Press (1973)
23. Lilly, D.K.: The representation of small-scale tubulence in numerical simulation experiments. In: H. H. Goldstine, Proceedings of IBM Scientific Computing Symposium on Environmental Sciences pp. 195–210 (1967)
24. Mémin, E.: Fluid flow dynamics under location uncertainty. Geophysical and Astrophysical Fluid Dynamics **108**(2), 119–146 (2014). DOI 10.1080/03091929.2013.836190
25. Métais, O., Lesieur, M.: Spectral large-eddy simulation of isotropic and stably stratified turbulence. Journal of Fluid Mechanics **239**, 157–194 (1992). DOI 10.1017/S0022112092004361
26. Mikulevicius, R., Rozovskii, B.L.: On Equations of Stochastic Fluid Mechanics. Trends in Mathematics. Birkhäuser, Boston, MA (2001). DOI doi.org/10.1007/978-1-4612-0167-0_15. In: Hida T., Karandikar R.L., Kunita H., Rajput B.S., Watanabe S., Xiong J. (eds) Stochastics in Finite and Infinite Dimensions.
27. Mikulevicius, R., Rozovskii, B.L.: Stochastic navier-stokes equations for turbulent flows. SIAM J. Mathematical Analysis **35**(5), 1250–1310 (2004). DOI doi.org/10.1137/S0036141002409167
28. Moser, R.D., Kim, J., Mansour, N.N.: Direct numerical simulation of turbulent channel flow up to re_τ=590. Physics of Fluids **11**(4), 943–945 (1999). DOI 10.1063/1.869966
29. Neves, W., Olivera, C.: Wellposedness for stochastic continuity equations with ladyzhenskaya–prodi–serrin condition. Nonlinear Differential Equations and Applications NoDEA **22**(5), 1247–1258 (2015). DOI 10.1007/s00030-015-0321-6
30. Nicoud, F., Ducros, F.: Subgrid-scale stress modelling based on the square of the velocity gradient tensor. Flow, Turbulence and Combustion **62**(3), 183–200 (1999). DOI 10.1023/A:1009995426001
31. Øksendal, B.: Stochastic Differential Equations. Springer-Verlag Berlin Heidelberg (2003). DOI 10.1007/978-3-642-14394-6
32. Oliveira, P.J., Issa, P.I.: An improved piso algorithm for the computation of bouyancy driven flows. Numerical Heat Transfers, Part B. Fundamentals **640**, 473 (2001)
33. Orszag, S.A.: Analytical theories of turbulence. Journal of Fluid Mechanics **41**(2), 363–386 (1970). DOI 10.1017/S0022112070000642
34. Piomelli, U.: Large-eddy and direct simulation of turbulent flows. CFD2001 - 9th Conférence Annuelle de la Société Canadienne de CFD (2001)
35. Pope, S.: Turbulent Flows. Cambridge University Press (2000)
36. Pope, S.B.: A lagrangian two-time probability density function equation for inhomogeneous turbulent flows. The Physics of Fluids **26**(12), 3448–3450 (1983). DOI 10.1063/1.864125

37. Resseguier, V., Mémin, E., Chapron, B.: Geophysical flows under location uncertainty, Part I: random transport and general models. Geophysical and Astrophysical Fluid Dynamics **111**(3), 149–176 (2017). DOI 10.1080/03091929.2017.1310210
38. Resseguier, V., Mémin, E., Chapron, B.: Geophysical flows under location uncertainty, Part II: quasi-geostrophy and efficient ensemble spreading. Geophysical and Astrophysical Fluid Dynamics **111**(3), 177–208 (2017). DOI 10.1080/03091929.2017.1312101
39. Resseguier, V., Mémin, E., Chapron, B.: Geophysical flows under location uncertainty, Part III: sqg and frontal dynamics under strong turbulence conditions. Geophysical and Astrophysical Fluid Dynamics **111**(3), 209–227 (2017). DOI 10.1080/03091929.2017.1312102
40. Resseguier, V., Mémin, E., Heitz, D., Chapron, B.: Stochastic modelling and diffusion modes for proper orthogonal decomposition models and small-scale flow analysis. Journal of Fluid Mechanics **826**, 888–917 (2017). DOI 10.1017/jfm.2017.467
41. Roman, F., Stipcich, G., Armenio, V., Inghilesi, R., Corsini, S.: Large eddy simulation of mixing in coastal areas. International Journal of Heat and Fluid Flow **31**(3), 327 – 341 (2010). DOI doi.org/10.1016/j.ijheatfluidflow.2010.02.006
42. Sagaut, P.: Large eddy simulation for incompressible flows. An introduction. Springer (2000)
43. Smagorinsky, J.: General circulation experiments with the primitive equations: I. the basic experiment. Mon. Weather Rev. **91**, 99 (1963)
44. Smith, C.R., Metzler, S.P.: The characteristics of low-speed streaks in the near-wall region of a turbulent boundary layer. Journal of Fluid Mechanics **129**, 27–54 (1983). DOI 10.1017/S0022112083000634